

ASSESSMENT OF EFFECTIVE-MEDIUM THEORIES OF ION-BEAM SPUTTERED $\text{Nb}_2\text{O}_5\text{-SiO}_2$ AND $\text{ZrO}_2\text{-SiO}_2$ MIXTURES

T. Tolenis ^a, M. Gaspariūnas ^a, M. Lelis ^b, A. Plukis ^a, R. Buzelis ^a, and A. Melninkaitis ^c

^a State Research Institute for Physical Sciences and Technology, Savanorių 231, LT-02300 Vilnius, Lithuania

E-mail: tomas.tolenis@ftmc.lt

^b Laser Research Center, Vilnius University, Saulėtekio 10, LT-10223 Vilnius, Lithuania

^c Lithuanian Energy Institute, Breslaujos 3, LT-44403 Kaunas, Lithuania

Received 15 July 2013; revised 24 October 2013; accepted 4 December 2013

Single-layer mixture coatings of $\text{ZrO}_2\text{-SiO}_2$ and $\text{Nb}_2\text{O}_5\text{-SiO}_2$ produced by the ion beam sputtering (IBS) deposition technique were investigated in detail. Effective medium approximation (EMA) models and two non-optical methods, namely Rutherford backscattering spectroscopy (RBS) and X-ray photoelectron spectroscopy (XPS) were applied for characterization of elemental composition of these films. The comparison of obtained results indicates discrepancies in atomic material concentrations. The reasons and potential sources of such discrepancies are discussed qualitatively and indicate limitations of optical models.

Keywords: optical coatings, composite thin films, ion beam sputtering

PACS: 42.79.Wc, 78.66.Sq, 81.15.Cd

1. Introduction

The IBS technology is well suited for production of high quality optical coatings and has some advantages compared to traditional evaporation techniques (electron-beam evaporation, ion-assisted deposition etc.) [1, 2]. Moreover, very complex designs can be realized by using the so-called “zone target” approach to mix the materials at an atomic level thus varying the refractive index in a continuous and well controllable manner [3–8]. Such IBS-based material mixing approach opens up completely new possibilities in optical and laser applications [9]. Furthermore, films of mixed materials are also known to exhibit very good physical features: reduced optical losses [10], better mechanical properties [11], and higher resistance to laser irradiation [12, 13]. However, before implementation of material mixing technology into the production of more advanced coatings, it is important to understand how the materials are mixed at a molecular level. For this purpose the effective medium approximation (EMA) based on the mixed particle model is frequently used to determine the volumetric fractions of materials in mixture coatings. The EMA approach is a relatively simple technique which is also sensitive to many factors and therefore sometimes results in non-accurate evaluations [14]. To evaluate the validity of EMA-based techniques for IBS coat-

ings we directly compare the obtained results with those of other non-optical techniques – Rutherford backscattering spectroscopy (RBS) and X-ray photoelectron spectroscopy (XPS). RBS is known to be an accurate way for determining atomic concentrations of elements [15, 16]. XPS is a surface chemical analysis technique that can be used to analyse elemental composition and chemistry of a material. Sometimes, as in this case, the material is measured after etching it with Ar^+ ions [17]. A direct comparison between optical and non-optical techniques can provide an important information about the shortcomings of EMA models and which approximation better describes the composition of the coatings.

2. Experiment

2.1. Preparation of thin film samples

All films were produced on the 25.4 mm diameter Fused Silica (FS) substrates. The ion-beam sputtering (IBS) technique was used for deposition of experimental coatings. Two vacuum pumps (cryopump and dry mechanical pump) were equipped for obtaining the vacuum of the base pressure of 3×10^{-4} Pa. To remove the impurity layer, the ion source was used for presputtering of the target before deposition. The target consisted of two metal plates: Zr (or Nb) for high refractive index material and Si for low refractive index material. During the process, oxygen gas was

supplied in the vacuum chamber to ensure complete oxidation of sputtered metal particles. The resulting working pressure was 3×10^{-2} Pa. Sputtering processes were controlled by a broadband optical monitor [18]. All films were of the same physical thickness – $6\lambda/4n$, where n is the refractive index of the coating. A total of nine different compositions were investigated with the silica fraction varying from 0 to 100% in desirable increments of 25%. The fraction of each material in the mixture was adjusted by sputtering appropriate parts of the target zones with the high energy ion beam during the deposition process. The coating with approximately 75% of high-refractive-index material was named the “high-index” mixture layer. Target coatings of 50% /50% and 25% /75% are named “medium-index” and “low-index” mixture layers, respectively. Later, the exact fractions were characterized by using effective medium theories.

3. Characterization of thin films

All the samples were measured in previous investigation by X-ray diffraction, angle-resolved and total integrated scattering, atomic force microscopy, and laser-induced damage threshold methods [19]. In addition, spectrophotometric data were also obtained. From reflectance and transmission measurements (Figs. 1(a, b)), refractive indices were modelled in a low-absorbance spectral region by using OptiChar characterization software [20]. The volumetric fractions $f_H = X$ in each (high refractive index) $_X$ (silica) $_{1-X}$ mixture system were analysed according to the so-called effective-medium theories. Maxwell Garnett (MG) [21], Bruggeman (BG) [22], and Lorentz–Lorenz (LL) [23, 24] mixing formulas [14] were used:

$$\text{MG: } \frac{\epsilon_{\text{eff}} - \epsilon_H}{\epsilon_{\text{eff}} + 2\epsilon_H} = (1 - f_H) \frac{\epsilon_{\text{eff}} - \epsilon_L}{\epsilon_{\text{eff}} + 2\epsilon_L}, \quad (1)$$

$$\text{BG: } f_H \frac{\epsilon_H - \epsilon_{\text{eff}}}{\epsilon_H + 2\epsilon_{\text{eff}}} + (1 - f_H) \frac{\epsilon_L - \epsilon_{\text{eff}}}{\epsilon_L + 2\epsilon_{\text{eff}}} = 0, \quad (2)$$

$$\text{LL: } \frac{\epsilon_{\text{eff}} - 1}{\epsilon_{\text{eff}} + 2} = f_H \frac{\epsilon_H - 1}{\epsilon_H + 2} + (1 - f_H) \frac{\epsilon_L - 1}{\epsilon_L + 2}, \quad (3)$$

where f_H is the volumetric material fraction of the higher-refractive-index material in a mixed layer, ϵ_{eff} , ϵ_H , and ϵ_L are the dielectric functions of the effective-medium (mixture) material, the high-refractive-index material, and the low-refractive-index material, respectively.

Different volumetric fractions are calculated by using different EMA theories. Additional measurements were necessary to claim which model exhibit

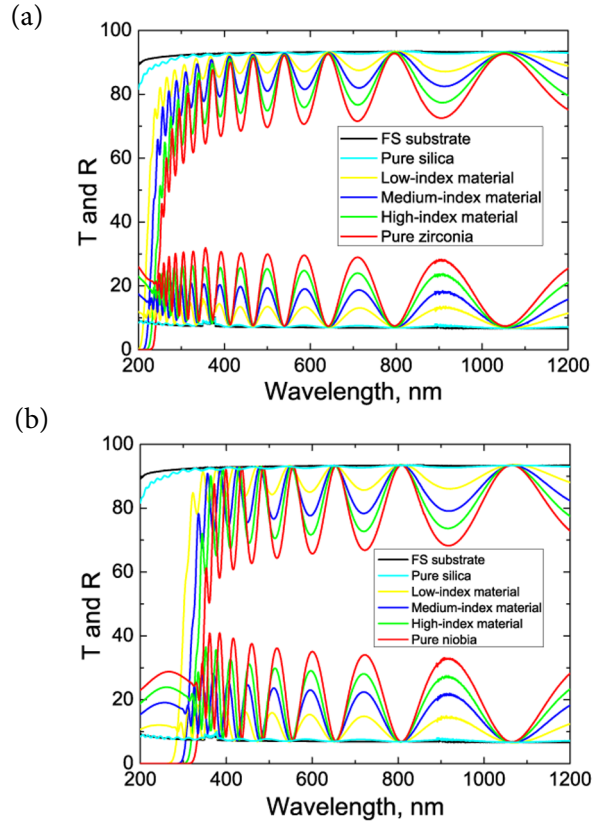


Fig. 1. (Colour online) Transmission and reflection spectrums of (a) zirconia-silica and (b) niobia-silica samples.

the best approximation. By this investigation authors continue their work to fully analyse and characterize mixed materials produced by IBS. For additional indication of elemental composition in mixtures, XPS and RBS techniques were chosen. Both of them are non-optical measurement techniques capable of accurate estimation of atomic concentrations in thin films.

3.1. Analysis of X-ray photoelectron spectroscopy

XPS measurements were performed with Versa-probe 5600 instrument manufactured by *Physical Electronics*, and data reduction was performed with Multipak software. Monochromated Al radiation (25 W, 15 kV) was focused into a $100 \mu\text{m}$ analysis area and used for measurements of the samples. The floating column Ar ion gun working at 500 V and rastering it over a $2 \times 2 \text{ mm}$ area was used for depth profiling. Sputtering by Ar ions was used for etching the sample to measure the in-depth profile. It was calibrated by SiO_2 standard and estimated to be at approximately 2:3 nm/min. Quantitative accuracy of the XPS method depends on several factors, and determination of its exact value is difficult

especially when ion gun sputtering is used. Considering all known factors, in this paper the accuracy of XPS is considered to be 10% of the value (15% for Si in mixtures).

The atomic concentration depth profiles of XPS measurements are shown in Fig. 2. Contamination was found on the surface of all the samples. The observed contamination was considered to be mainly hydrocarbons from the atmosphere. Hydrogen cannot be measured with the XPS method, but carbon was detectable in all the samples. The etching was performed in 0.5 min steps and after the first step of etching, contamination layers were already fully removed from the thin films. An exception was noticed in the “high-index” zirconia-silica mixture. Contamination was examined through all depth profiles. Additional investigation is necessary to explain this observation. To neglect the influence of contamination and sputtering process, atomic concentrations of films were obtained after the first step of sputtering. Data were recalculated by neglecting carbon.

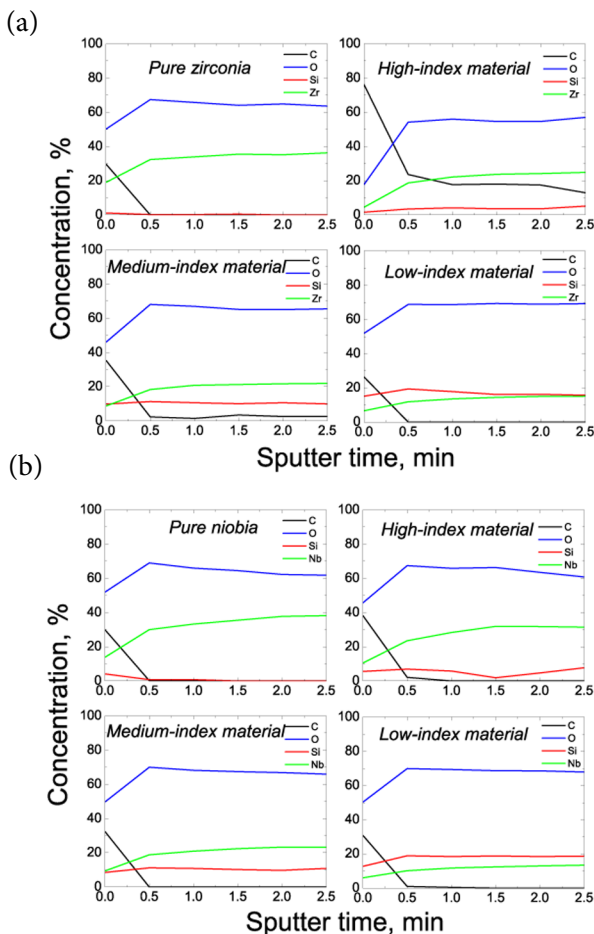


Fig. 2. (Colour online) XPS atomic concentration depth profiles of (a) zirconia-silica and (b) niobia-silica samples.

3.2. Analysis of Rutherford backscattering data

Two sets of single-layer coatings were also analysed using a linear particle accelerator Tandetron 4110A [25]. A proton beam of 1.4 and 1.8 MeV energy was collimated to 1.5 mm spot diameter. As a universal vacuum chamber was adapted for RBS experiments, one stationary angle $\theta = 135^\circ$ was available for experiments in Cornell geometry [26]. RBS spectra were iteratively modelled using the RBXN code [26–28]. Typical RBS spectra of single-layer optical coatings and theoretical calculations (black line in Figures) are presented in Figs. 3(a, b). The charge of 1.7–2.3 and 0.9–1.0 μC was collected on the samples when the energy of the beam reached 1.4 and 1.8 MeV, respectively. The results of atomic concentrations measured by the RBS technique are summarized in Figs. 4(a) and 5(a). No contamination was noticed on the samples, because it is difficult to measure the consistency of carbon or hydrogen by the RBS method. Nuclears of those elements are too small to cause backscattering.

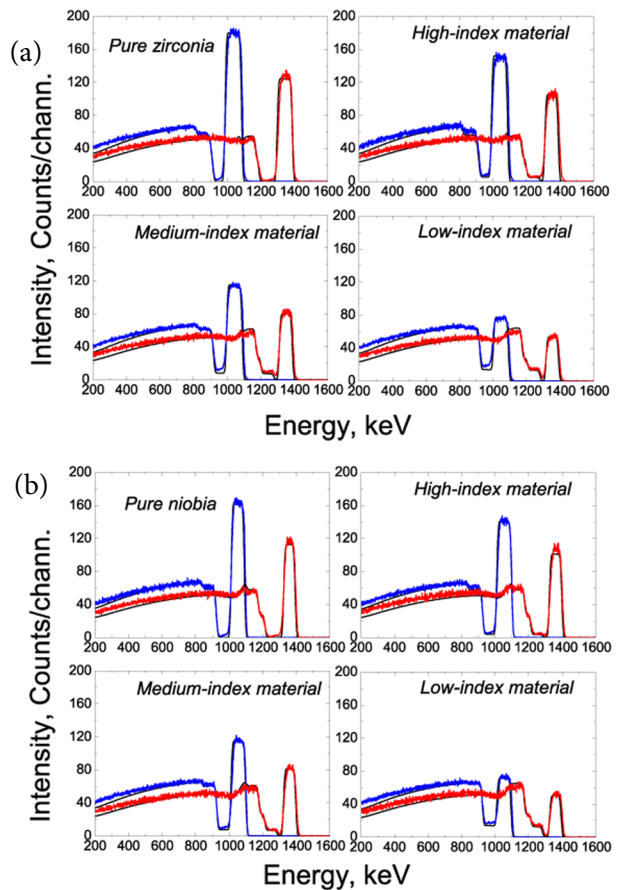


Fig. 3. (Colour online) Set of (a) zirconia-silica and (b) niobia-silica samples. Measured (blue 1.4 MeV, higher peaks, red 1.8 MeV, lower peaks) and modelled (thin black) RBS curves of coatings.

3.3. Analysis of spectrophotometric data

In order to compare obtained results from EMA volumetric fractions with RBS and XPS data, an estimation of molar atomic concentrations is done by considering an ideal stoichiometric ratio in pure zirconia, silica (Zr, Si:O = 1:2), and niobia (Nb:O = 2:5) coatings [2]. Molar atomic concentrations for each sample were calculated by using the system of equations:

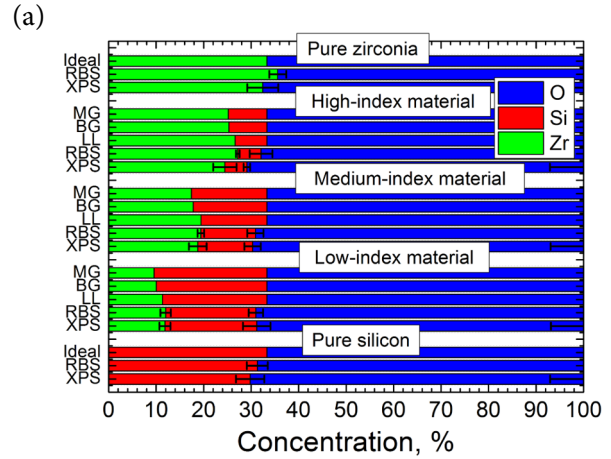
$$\begin{cases} \frac{V_X}{V_X + V_{1-X}} = f_H \\ s_{\text{metal}} + s_{\text{Si}} + s_{\text{O}} = 100\% , \\ V_{\text{po}} = \frac{s_{\text{po}} M}{N_{\text{Ap}}} \end{cases} \quad (4)$$

where f_H is the same volumetric fraction of pure oxide in the mixture obtained from EMA, V_X and V_{1-X} are the volumes of high-refractive-index material and silica, respectively. Symbol s represents a molar fraction of: metal – niobium or zirconium, Si – silicon, and O – oxygen. V_{po} is a volume of any individual pure oxide material, s_{po} is molar fraction, M is a molar mass, N_A is an Avogadro's number, and ρ is a mass density of material. For IBS coatings the mass density is close to that of bulk materials [29]. By solving the equations of system (4), we are able to estimate molar atomic fractions for every group of atoms in all films.

4. Results and discussion

Figures 4(a) and 5(a) illustrate the results of all three different methods for obtaining atomic concentrations of mixed materials. From EMA estimations it was difficult to claim which of the models corresponds to the real situation. Other methods were used to compare concentrations with optical approximations and for determining the correct model. Usually the RBS method can be trusted for precise determination of atomic concentrations of materials [25–28]. Because of precision, this technique was used as a comparison for EMA and as an indicator of the real situation. As another non-optical technique, XPS method was used to estimate atomic concentrations in depth profiles of mixtures.

By neglecting the influences of surface contaminations and sputtering, it was showed that results obtained by the XPS technique are in agreement with RBS measurements. A few discrepancies are found in ZrO_2 - SiO_2 mixtures, which still requires additional investigation. For a pure zirconia sample, RBS measurement exhibited incomplete oxidation with stoichiometric ratio of 1:1.82 instead of



(b)

Coating	Element			
	Model	Zr	Si	O
Low refractive index	LL	1.06	0.86	1.03
	BG	1.20	0.82	1.03
	MG	1.26	0.80	1.03
Medium refractive index	LL	1.00	0.83	1.04
	BG	1.09	0.74	1.04
	MG	1.11	0.72	1.04
High refractive index	LL	1.02	0.73	1.02
	BG	1.07	0.61	1.02
	MG	1.08	0.60	1.02

Fig. 4. (Colour online) (a) A direct comparison of atomic fractions within zirconiasilica samples. (b) A table of (RBS data)/(EMA data) ratios for Zr, Si, and O elements in zirconia-silica mixes.

ideal 1:2. XPS measurements showed the result of 1:2.08 which is within the error bars of ideal stoichiometry. In a pure niobia sample, both non-optical techniques detected incomplete oxidation. The RBS technique showed that for a pure niobia sample the ratio of niobium and oxygen was 2:4.8, while XPS showed 2:4.6. Controversial results were also shown in the measurements of pure silica. The ratio obtained by the RBS technique of silica with oxygen was 1:2.2, when XPS measured 1:2.4. The difference can be caused by the difficulty of obtaining exact concentration with the RBS method. The contrast of substrate and the thin film diminishes when they are of the same material (SiO_2). All three samples were considered reference samples having the ideal stoichiometry for EMA analysis.

In Nb_2O_5 - SiO_2 mixes, the Lorentz-Lorenz model exhibits a reasonably good estimation of the volumetric fractions with respect to data of non-optical methods. For a niobium element, the ratios between LL model and RBS measurements were within 6%, when BG and

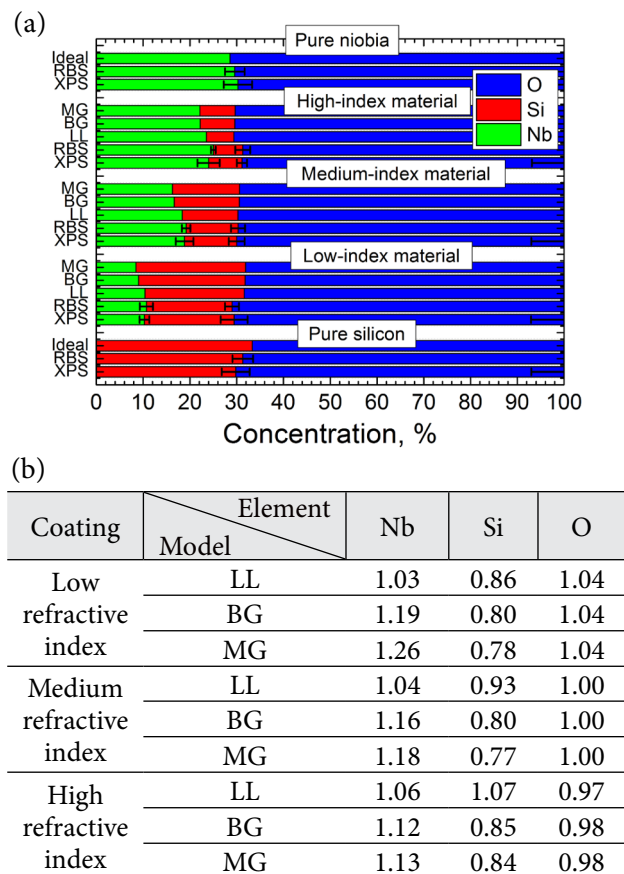


Fig. 5. (Colour online) (a) A direct comparison of atomic fractions within niobia silica samples. (b) A table of (RBS data)/(EMA data) ratios for Nb, Si, and O elements in niobia-silica mixes.

MG models showed the mismatches within 19% and 26%, respectively (Fig. 5(b)). For a silicon element, the ratios using LL model were within 14%. For BG and MG models, the mismatches were 20% and 23%, respectively. For an oxygen element, all models showed the ratio within 4%. This is in good agreement with conclusions obtained by Janicki et al. [14]. Very similar, but less accurate results are observed in zirconia-silica mixtures. For a zirconium element, the ratios between LL model and RBS measurements were within 6%, when BG and MG models showed the mismatches within 20% and 26%, respectively (Fig. 4(b)). For a silicon element, the ratios using the LL model were within 27%. For BG and MG models, the mismatches were 39% and 40%, respectively. For an oxygen element, all models showed the ratio within 4%. A pure zirconia sample also has a poly-crystalline nano-structure, while other samples are amorphous [19]. Mixing zirconia in different phases with silica may result in additional discrepancies when using EMA models. Besides the crystallinity, a pure sputtered ZrO_2 material tends to have an increased stress compared to mixtures with

SiO_2 [11]. The increased stress influences the refractive index, as have been shown by Stenzel et al. [30]. The reason for deviations is also the increased light scattering caused by nano-crystallinity [19] in a pure zirconia sample as the reference sample. Refractive index modelling was influenced by light losses, and permittivity of ZrO_2 was different in pure zirconia and its mixture with silica. In a high-index material mixture of ZrO_2-SiO_2 , RBS measurements show a different result than XPS data do. The sample contains more contamination than other samples, which can influence the XPS results. Additional measurements are required for this sample.

By considering RBS and XPS data it is evident that discrepancies arise due to poor stoichiometry, contamination, and different structures of materials in the coatings. This allows us to conclude that the LL EMA model is useful for quick estimation of material concentrations in IBS metal-oxide mixtures when the oxidation is complete, reference samples are of the same material as mixtures, and good stoichiometry is observed. However, when it is not the case, large deviations are possible and for absolute measurements other supplementary techniques are needed.

5. Conclusion

The applicability of Lorentz-Lorenz, Bruggaman, and Maxwell-Garnet effective medium approximation models for estimation of material fractions was studied experimentally in ion beam sputtered oxide mixture coatings. Estimations of used EMA models exhibited slightly controversial results. After comparing them to the RBS and XPS measurements, it was evident that the Lorentz-Lorenz model provided a more reliable estimation of elemental composition than BG and MG models did. This was observed in case of all niobia-silica and zirconia-silica mixtures. Small deviations for the LL model arise due to refractive index differences in zirconia as a reference sample and mixtures with silica. Additional discrepancies may also arise due to the light scattering losses caused from rough crystalline structure or mass density variations in mixed coating. In niobia-silica mixtures incomplete oxidation was observed, which may also distort the results of effective medium approximations. This allows us to conclude that in situations where an ideal stoichiometric ratio is violated, none of EMA techniques are able to describe volumetric fractions without using supplementary techniques. Also, larger deviations from the data of non-optical methods are more significant in a high-index zirconia-silica mixture. An explanation of this discrepancy requires additional investigation.

Acknowledgement

This research has been supported by the Lithuanian Agency for Science, Innovation and Technology grant EIGULYS (Project No. 31V-140). Authors are also thankful to Simonas Kičas for assistance in sample preparation

References

- [1] A.F. Stewart, S.M. Lu, M.M. Tehrani, and C. Volk, Ion beam sputtering of optical coatings, *Proc. SPIE* **2114**, 662–677 (1994).
- [2] P.J. Martin, Ion-based methods for optical thin film deposition, *J Mater. Sci.* **21**, 1–25 (1986), 10.1007/BF01144693
- [3] Ch.-Ch. Lee, Ch.-J. Tang, J.-Ch. Hsu, and J.-Y. Wu, Rugate filter made with composite thin film by ion beam sputtering, in: *Optical Interference Coatings*, page ThD10 (Optical Society of America, 2004).
- [4] J. Zhang, M. Fang, Y. Jin, and H. He, Narrow linewidth filters based on rugate structure and antireflection coating, *Thin Solid Films* **520**(16), 5447–5450 (2012).
- [5] S. Lange, H. Bartzsch, P. Frach, and K. Goedicke, Pulse magnetron sputtering in a reactive gas mixture of variable composition to manufacture multilayer and gradient optical coatings, *Thin Solid Films* **502**(1–2), 29–33 (2006).
- [6] G. Abromavičius, R. Buzelis, R. Drazdys, K. Juškevičius, S. Kičas, T. Tolenis, J. Mirauskas, M. Ščiuka, V. Sirutkaitis, and A. Melninkaitis, Optical resistance and spectral properties of anti-reflective coatings deposited on LBO crystals by ion beam sputtering, *Lith. J. Phys.* **51**(4), 303–308 (2011).
- [7] W.E. Johnson and R.L. Crane, Introduction to rugate filter technology, *Proc. SPIE* **2046**, 88–108 (1993).
- [8] V. Pervak, A.V. Tikhonravov, M.K. Trubetskov, J. Pistner, F. Krausz, and A. Apolonski, Band filters: two-material technology versus rugate, *Appl. Opt.* **46**(8), 1190–1193 (2007).
- [9] R.R. Willey, *Practical Design and Production of Optical Thin Films*, 2nd ed. (Marcel Dekker, 2005).
- [10] Sh. Chao, W.-H. Wang, and Ch.-Ch. Lee, Low-loss dielectric mirror with ion-beam-sputtered TiO_2 - SiO_2 mixed films, *Appl. Opt.* **40**(13), 2177–2182 (2001).
- [11] B.J. Pond, J.I. DeBar, C.K. Carniglia, and T. Raj, Stress reduction in ion beam sputtered mixed oxide films, *Appl. Opt.* **28**(14), 2800–2805 (1989).
- [12] M. Jupé, M. Lappschies, L. Jensen, K. Starke, and D. Ristau, Applications of mixture oxide materials for fs optics, in: *Optical Interference Coatings*, page TuA6 (Optical Society of America, 2007).
- [13] D. Nguyen, L.A. Emmert, I.V. Cravetchi, M. Mero, W. Rudolph, M. Jupé, M. Lappschies, K. Starke, and D. Ristau, $\text{Ti}_x\text{Si}_{1-x}\text{O}_2$ optical coatings with tunable index and their response to intense subpicosecond laser pulse irradiation, *Appl. Phys. Lett.* **93**, 261903(2008).
- [14] V. Janicki, J. Sanchoparramon, and H. Zorc, Refractive index profile modelling of dielectric inhomogeneous coatings using effective medium theories, *Thin Solid Films* **516**(10), 3368–3373 (2008).
- [15] K. Drogowska, Z. Tarnawski, A. Brudnik, E. Kusior, M. Sokołowski, K. Zakrzewska, A. Reszka, N.-T.H. Kim-Ngan, and A.G. Balogh, RBS, XRR and optical reflectivity measurements of Ti-TiO₂ thin films deposited by magnetron sputtering, *Mater. Res. Bull.* **47**(2), 296–301 (2012).
- [16] R. Vlastou, E. Fokitis, M. Kokkoris, S. Kossionides, G. Koubouras, and R. Grotzschel, Characterization of multilayer thin film optical filters using RBS, *AIP Conf. Proc.* **576**(1), 436–439 (2001).
- [17] M. Alvisi, L. Mirengi, L. Tapfer, A. Rizzo, M.C. Ferrara, S. Scaglione, and L. Vasanelli, Structural and chemical investigation of surface and interface of multilayer optical coatings deposited by DIBS, *Appl. Surf. Sci.* **157**(1–2), 52–60 (2000).
- [18] D. Ristau, H. Ehlers, T. Gross, and M. Lappschies, Optical broadband monitoring of conventional and ion processes, *Appl. Opt.* **45**(7), 1495–1501 (2006).
- [19] A. Melninkaitis, T. Tolenis, L. Mažulė, J. Mirauskas, V. Sirutkaitis, B. Mangote, X. Fu, M. Zerrad, L. Gallais, M. Commandré, S. Kičas, and R. Drazdys, Characterization of zirconia- and niobia-silica mixture coatings produced by ion-beam sputtering, *Appl. Opt.* **50**(9), C188–C196 (2011).
- [20] Optilayer, 1996, <http://www.optilayer.com>, last accessed: 13/11/2012.
- [21] J.C. Maxwell Garnett, Colours in metal glasses and in metallic films, *Phil. Trans. R. Soc. Lond. A* **203**(329–371), 385–420 (1904).
- [22] D.A.G. Bruggeman, Berechnung verschiedener physikalischer Konstanten von heterogenen Substanzen. i. Dielektrizitätskonstanten und Leitfähigkeiten der Mischkörper aus isotropen Substanzen, *Annalen der Physik* **416**(7), 636–664 (1935).
- [23] H.A. Lorentz, Ueber die Beziehung zwischen der Fortpflanzungsgeschwindigkeit des Lichtes und der Körperdichte, *Annalen der Physik* **245**(4), 641–665 (1880).
- [24] L. Lorenz, Ueber die Refraktionsconstante, *Annalen der Physik* **247**(9), 70–103 (1880).
- [25] M. Gaspariūnas, G. Gervinskas, V. Kovalevskij, R. Plukienė, Š. Vaitekoniš, V. Levenets, and A. Plukis, Proton and ion microbeam collimation for irradiation of biological samples in air, *Lith. J. Phys.* **50**, 363–368 (2010).
- [26] M. Mayer, SIMNRA, a simulation program for the analysis of NRA, RBS and ERDA, *AIP Conf. Proc.* **475**(1), 541–544 (1999).

- [27] E. Rauhala, N.P. Barradas, S. Fazinic, M. Mayer, E. Szilágyi, and M. Thompson, Status of ion beam data analysis and simulation software, Nucl. Instr. Methods B **244**(2), 436–456 (2006).
- [28] N.P. Barradas, K. Arstila, G. Battistig, M. Bianconi, N. Dytlewski, C. Jeynes, E. Kótai, G. Lulli, M. Mayer, E. Rauhala, E. Szilágyi, and M. Thompson, International Atomic Energy Agency intercomparison of ion beam analysis software, Nucl. Instr. Methods B **262**(2), 281–303 (2007).
- [29] S.G. Yoon, Y.T. Kim, H.K. Kim, M.J. Kim, H.M. Lee, and D.H. Yoon, Comparison of residual stress and optical properties in Ta₂O₅ thin films deposited by single and dual ion beam sputtering, Mater. Sci. Eng. B **118**(1–3), 234–237 (2005); EMRS 2004, Symposium D: Functional Oxides for Advanced Semiconductor Technologies.
- [30] O. Stenzel, S. Wilbrandt, N. Kaiser, M. Vinichenko, F. Munnik, A. Kolitsch, A. Chuvilin, U. Kaiser, J. Ebert, S. Jakobs, and A. Kaless, The correlation between mechanical stress, thermal shift and refractive index in HfO₂, Nb₂O₅, Ta₂O₅ and SiO₂ layers and its relation to the layer porosity, Thin Solid Films **517**(21), 6058–6068 (2009).

EFEKTYVIOSIOS TERPĖS TEORIJŲ ĮVERTINIMAS Nb₂O₅-SiO₂ IR ZrO₂-SiO₂ MIŠINIuose, UŽGARINTuose JONAPLUOŠČIO DULKINIMO TECHNOLOGIJA

T. Tolenis^a, M. Gaspariūnas^a, M. Lelis^b, A. Plukis^a, R. Buzelis^a, A. Melninkaitis^c

^a Valstybinis mokslinių tyrimų institutas Fizinių ir technologijos mokslų centras, Vilnius, Lietuva

^b Vilniaus universiteto Lazerinių tyrimų centras, Vilnius, Lietuva

^c Lietuvos energetikos institutas, Kaunas, Lietuva

Santrauka

Darbe išsamiai ištirtos vienasluoksnės ZrO₂-SiO₂ ir Nb₂O₅-SiO₂ dangos, užgarintos naudojant jonapluoščio dulkinimo technologiją. Nustatant cheminę sudėtį buvo pasinaudota trimis nepriklausomomis metodikomis: efektyviosios terpės aproksimacija, Rezerfordo atgalinės sklaidos spektroskopija ir Rentgeno spindulių fotoelektronų spektroskopija. Tiesiogiai lyginant gautus

rezultatus buvo pastebėta metodikų netikslumų. Tokių netikslumų priežastys atsiranda dėl netobulos stochiometrijos, bandinių užterštumo ir skirtingos medžiagos būsenos dangose. Įvertinta, kad Lorencio-Lorenzo modelis tinka nustatyti greitą ir apytikslią medžiagų koncentraciją, bet atliekant tikslesnę analizę būtini kiti metodai.